Transport and magnetic properties of a Mott-Hubbard system whose bandwidth and band filling are both controllable: $R_{1-x}Ca_xTiO_{3+y/2}$

T. Katsufuji, Y. Taguchi, and Y. Tokura
Department of Applied Physics, University of Tokyo, Tokyo 113, Japan
(Received 14 May 1997)

Transport and magnetic properties of $R_{1-x}Ca_xTiO_{3+y/2}$ have been systematically investigated varying the one-electron bandwidth (W) and the band filling ($n=1-\delta$), which can be controlled by the R-dependent lattice distortion and by the Ca content x and/or oxygen offstoichiometry y ($\delta=x+y$), respectively. The end compound $RTiO_3$ is a $3d^1$ Mott-Hubbard insulator and its charge-gap magnitude increases with decreasing ionic radius of R, i.e., an increase of electron correlation (U/W) in proportion with $(U/W)-(U/W)_c$, where $(U/W)_c$ is the critical value for the (hypothetical) $n=1$ Mott transition. Such a Mott insulator is transformed to a correlated metal by substitution of R with Ca (hole doping), and the nominal hole concentration required for the insulator-metal transition (δ_c) increases in proportion with $(U/W)-(U/W)_c$. Concerning magnetism, $RTiO_3$ with $R=$La, Pr, Nd, and Sm, shows the antiferromagnetic ordering and its Néel temperature (T_N) decreases with smaller R. T_N also decreases with Ca doping, but remains finite up to the metal-insulator phase boundary. On the basis of these results, electronic phase diagrams are derived for a series of titanates as an electron-correlated system with changes of two parameters, i.e., the strength of electron correlation and band filling. Possible origins of the insulating state with finite hole doping are also discussed in terms of the kinetic energy of doped carriers in the Mott-Hubbard insulator. [S0163-1829(97)05640-3]

I. INTRODUCTION

In $3d$ transition-metal oxides, strong electron-electron interaction often localizes conduction electrons, and the system becomes an insulator (a Mott insulator).[1] In some cases, a transition between a metal and a Mott insulator is observed by a slight change of some parameters (a Mott transition). A famous example that shows such a transition is V_2O_3,[2] where a metal-insulator transition at the lowest temperature occurs with the application of pressure. This metal-insulator transition can be interpreted as one induced by changes of the bandwidth of the conduction band arising from changes of a lattice constant (a bandwidth-control Mott transition). On the other hand, metal-insulator transitions observed in cuprate superconductors are categorized another way. For example, La_2CuO_4 is a Mott insulator with a Cu $3d^9$ electron configuration, and becomes metallic with hole doping by the substitution of the trivalent La ion with a divalent Sr ion.[3] In contrast to the case of pressurized V_2O_3, the metal-insulator transition of $La_{2-x}Sr_xCuO_4$ is induced by changes of the band filling of the conduction band (a filling-control Mott transition).[4]

Recently, $R_{1-x}A_xTiO_3$ (R being a trivalent rare earth, and A a divalent alkaline earth) has been studied as a prototypical three-dimensional electron-correlated system.[5–19] A unique feature of this system is that both the bandwidth and the band filling can be chemically controlled: The end compound $RTiO_3$, where the Ti atom is in the $3d^1$ electron configuration, is a Mott insulator irrespective of the species of the rare earth R.[5,6] With a smaller ionic radius of R, the lattice structure becomes more distorted, and the Ti-O-Ti bond angle decreases, with a greater departure from 180°. Since the conduction band of these compounds is composed of the Ti $3d$ (t_{2g}) and oxygen $2p$ orbitals, such a decrease of the Ti-O-Ti bond angle leads to a decrease of the one-electron bandwidth of the conduction band.[7] On the other hand, the substitution of the trivalent R ion by the divalent A ion decreases the number of electrons per Ti site (n) from 1 (nominal hole doping), and drives the system metallic.[8–12] There have been various studies on this system, but few systematic studies of transport and magnetic properties with changes of both the two parameters, i.e., bandwidth and band filling.

In this paper, we report a systematic investigation of $R_{1-x}Ca_xTiO_{3+y/2}$, with $R=$La, Pr, Nd, Sm, and Y, with a finely controlled Ca concentration x and oxygen offstoichiometry y. From this study, we can obtain detailed information about the electronic and magnetic structures of this system for wide ranges of the two parameters, bandwidth and band filling. Such a study is expected to clarify generic features of three-dimensional, doped, Mott-Hubbard systems. We also focus on the critical behavior of the metal-insulator phase boundary of this system.

The format of this paper is as follows: In Sec. II details of the sample preparation and measurements are described. In Sec. III, we describe the calculation of the bandwidth of the conduction band, which characterizes the respective compounds. Sections IV and V show the experimental results of resistivity and magnetization, respectively, and Sec. V presents an electronic phase diagram of this system in a space of bandwidth, band filling, and temperature. In Sec. VI some features observed in the vicinity of the metal-insulator phase boundaries are presented. In Sec. VII we discuss a possible origin of the insulating state with finite hole concentration, and Sec. VIII is devoted to a summary of the paper.

II. EXPERIMENT

All the samples investigated in this study were prepared by the floating zone method, similarly to previous work.[11]

TABLE I. Ti-O-Ti bond angle and bandwidth of the conduction band of $R\mathrm{TiO_3}$. The values of the bond are from Ref. 13 except for $\mathrm{PrTiO_3}$, whose bond angles (in parentheses) are obtained by the interpolation of $\mathrm{LaTiO_3}$ and $\mathrm{NdTiO_3}$ using their tolerance factors (see Ref. 21). O(1) and O(2) refer to the oxygens at two different sites of the $\mathrm{GdFeO_3}$ structure. W is the full width of the conduction band calculated with the tight-binding approximation. $\widetilde{W}$ is the ratio of W of each $R\mathrm{TiO_3}$ to that of $\mathrm{LaTiO_3}$.

	La	Pr	Nd	Sm	Y
Ti-O(1)-Ti bond angle (degree)	157.5	(152.8)	150.7	146.8	140.3
Ti-O(2)-Ti bond angle (degree)	156.9	(152.3)	150.3	147.0	143.7
W (eV)	2.45	2.33	2.27	2.16	2.04
$\widetilde{W}$	1	0.95	0.93	0.88	0.83

The starting materials are $R_2\mathrm{O_3}$ (R=La, Pr, Nd, Sm, and Y), $\mathrm{TiO_2}$, Ti, and $\mathrm{CaTiO_3}$. $\mathrm{CaTiO_3}$ was synthesized by firing $\mathrm{CaCO_3}$ and $\mathrm{TiO_2}$ in air at 1000 C° for 24 h. Stoichiometric amount of sources for $R_{1-x}\mathrm{Ca}_x\mathrm{TiO_3}$, which had been well dried in advance, were mixed and pressed into rods with ~5-mm diameter. To keep the stoichiometry of oxygen, we omitted a sintering procedure, and directly melted the pressed bar with use of a floating zone furnace equipped with two halogen lamps and ellipsoidal mirrors. Atmosphere in the furnace during the crystal growth was varied to control the oxygen offstoichiometry of the samples (y), which was determined by thermogravimetric analysis. The stoichiometric $R\mathrm{TiO_{3.00}}$ could be obtained in a gas flow of 30% $\mathrm{H_2/Ar}$, whereas the melting in a gas flow of Ar (6N) often results in excess oxygen ($y/2=0.04$ as a typical value). We assume that the ratio of R, Ca, and Ti does not change from the starting ratio. Thus the nominal hole concentration δ is given by $x+y$.

X-ray powder diffraction was measured which showed that the crystal structure of all the samples investigated here is the $\mathrm{GdFeO_3}$ type. Resistivity measurements were carried out by the conventional four-probe technique using indium as an electrode. Magnetization measurement were performed using a superconducting quantum interference device magnetometer.

III. CALCULATION OF BANDWIDTH

The conduction band of this system is composed of Ti $3d$ t_{2g} and O $2p$ π orbitals, and its bandwidth is governed by the Ti-O-Ti bond angle. Complete structural parameters were previously determined for $R\mathrm{TiO_3}$ in Ref. 13, and, with use of their data, the one-electron bandwidth of the conduction band for $R\mathrm{TiO_3}$ can be calculated by a tight-binding model, where the Hamiltonian matrix, based on the Harrison's parametrization[20] taking account of Ti $3d$ t_{2g} and O $2p$ orbital with $\mathrm{GdFeO_3}$ lattice distortion is diagonalized. Details of the calculation are shown in Ref. 7. The Ti-O-Ti bond angle and the full width of the conduction band (W) from the calculation are listed in Table I. $\widetilde{W}$ is the ratio of W of each $R\mathrm{TiO_3}$ to that of $\mathrm{LaTiO_3}$. Among these, the minimal bandwidth of $\mathrm{YTiO_3}$ is 83% of the maximal one of $\mathrm{LaTiO_3}$.

Ca doping may also induce a change in the Ti-O-Ti bond angle, and consequently in the bandwidth of the conduction band. Since to our knowledge the Ti-O-Ti bond angle of $R_{1-x}\mathrm{Ca}_x\mathrm{TiO_{3+y/2}}$ with a finite value of x has not been determined so far experimentally we estimated the change of a tolerance factor[21] instead of the bond angle. The tolerance factor of $\mathrm{LaTiO_3}$ is 0.95, and that of $\mathrm{YTiO_3}$ is 0.89; the difference is ~6%. On the other hand, the factors of $\mathrm{NdTiO_3}$ and $\mathrm{Nd_{0.8}Ca_{0.2}TiO_3}$ are 0.92 and 0.93, respectively; the difference is only ~1%. Thus, as long as properties in the small-x region are discussed, the change of the bond angle with Ca doping is negligible, and from now on we ignore the change of the bandwidth with Ca doping.

In the spirit of the Hubbard model, the electron-correlation strength is given by U/W, where U is the on-site Coulomb repulsion energy. Since the U value can be viewed as constant among the $R\mathrm{TiO_3}$ series, we use the value of $\widetilde{W}^{-1}$ in the following sections to represent the electron-correlation strength below.

IV. TRANSPORT PROPERTIES

Figure 1 shows the temperature dependence of the resistivity for $R_{1-x}\mathrm{Ca}_x\mathrm{TiO_{3+y/2}}$, with R=La, Pr, Nd, and Sm, and with various hole concentrations. Results for $\mathrm{Y_{1-x}Ca}_x\mathrm{TiO_3}$ (not shown) have already been published in Ref. 10. For any R, the change of resistivity with hole doping is similar: With an increase of hole concentration δ, the temperature dependence of the resistivity varies from insu-

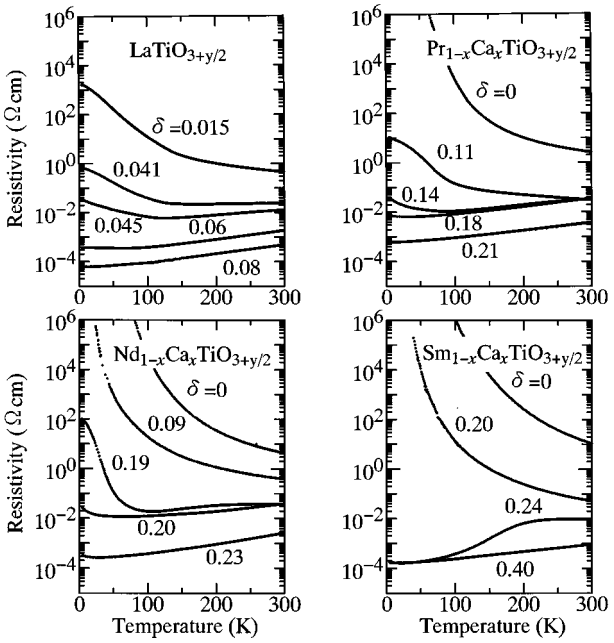

FIG. 1. Temperature dependence of resistivity in crystals of $R_{1-x}\mathrm{Ca}_x\mathrm{TiO_{3+y/2}}$ for R=La, Pr, Nd, and Sm with various hole concentrations $\delta=x+y$. The result of R=Y is shown in Ref. 10.

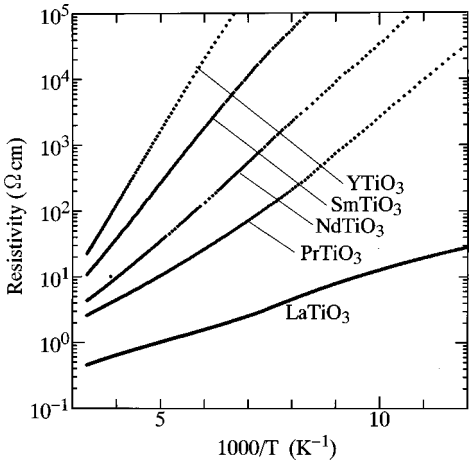

FIG. 2. Resistivity on a logarithmic scale vs the inverse of temperature for $R\mathrm{TiO}_3$.

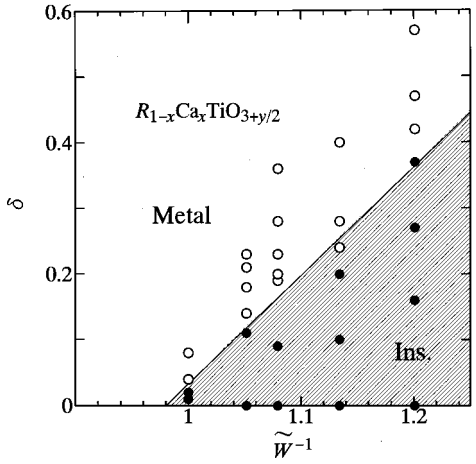

FIG. 4. Insulating crystals (closed circles) and metallic ones (open circles) are plotted in $\widetilde{W}^{-1}$-δ space. For the definition of ''metallic'' and ''insulating'' crystals, see text. The solid line is the guide to the eyes, representing a linear relation that separates the space into insulating and metallic regions.

lating with thermal activation to metallic ($d\rho/dT$ being positive). However, there are several R-dependent features. (1) The resistivity for the end compound ($\delta=0$) increases from $R=$La to Sm (with a decrease of W). (2) The hole concentration that is required to make the system metallic increases from La to Sm. For example, $\delta=0.08$ is sufficient to make LaTiO_3 metallic, whereas the sample with $\delta=0.09$ is still insulating for $\mathrm{Nd}_{1-x}\mathrm{Ca}_x\mathrm{TiO}_{3+y/2}$.

To discuss the former point more quantitatively, in Fig. 2 we show an Arrhenius plot of the resistivity for the end compound $R\mathrm{TiO}_3$. All the data approximately follow the activation-type function $\rho(T)=\rho_0\exp(\Delta_{\mathrm{act}}/k_BT)$, where the activation energy Δ_{act} (the slope of the line) decreases from YTiO_3 to LaTiO_3. We estimate the Δ_{act} value of $R\mathrm{TiO}_3$ from the high-temperature part, and plot $2\Delta_{\mathrm{act}}$ as a transport gap against the inverse bandwidth $\widetilde{W}^{-1}$ in Fig. 3. The $2\Delta_{\mathrm{act}}$ value decreases linearly with the decrease of $\widetilde{W}^{-1}$. The solid line in Fig. 3 is the result of a least-square fitting of the data with a linear function. This fitting suggests that $2\Delta_{\mathrm{act}}$ becomes zero at a finite value of $\widetilde{W}^{-1}$ ($\sim$0.95). We have observed a similar $\widetilde{W}^{-1}$ dependence of the energy gap in optical conductivity spectra for $R\mathrm{TiO}_3$.[5] These experimental results indicate that the relation between the magnitude of the Mott-Hubbard gap (E_g) depends on the electron-correlation strength (U/W) in such a way that $E_g\propto U/W-(U/W)_c$.[22] Here $(U/W)_c$ is a hypothetical point for a Mott transition with $n=1$ ($\delta=0$) filling. We note that recent calculations of the Hubbard model at infinite dimensions[23] confirmed a metal-insulator transition for $n=1$ with a finite value of U/W, and quantitatively explained such a U/W dependence of E_g.[24]

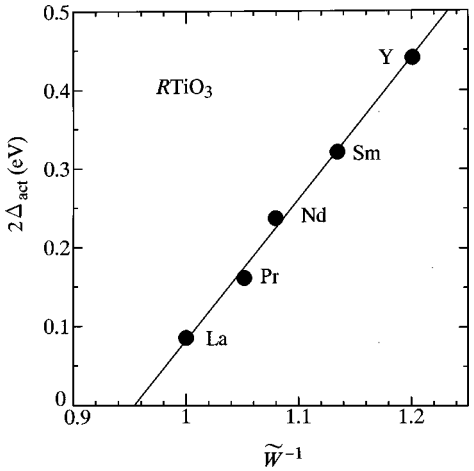

FIG. 3. $2\Delta_{\mathrm{act}}$ vs $\widetilde{W}^{-1}$ for $R\mathrm{TiO}_3$. Δ_{act} is the activation energy of resistivity and $\widetilde{W}$ is the bandwidth of $R\mathrm{TiO}_3$ normalized to that of LaTiO_3. The solid line is the result of least-square fitting with a linear function.

The critical R dependence of the transport properties also emerges when hole doping (δ) into the end compound, $R\mathrm{TiO}_3$, causes the insulator-metal transition. In Fig. 4, insulating and metallic samples are plotted by closed and open circles, respectively, in a $\widetilde{W}^{-1}$-δ space. Here we define an insulator as a sample whose $d\rho/dT$ is negative over the whole temperature range. It is clear from this figure that the nominal hole concentration that is needed to cause the insulator-metal transition (δ_c) increases with increase of electron-correlation strength $\widetilde{W}^{-1}$. The $\widetilde{W}^{-1}$ dependence of δ_c appears to be a linear function, as indicated by the solid line. Moreover, the $\widetilde{W}^{-1}$ value at which δ_c becomes zero approximately coincides with the one at which $2\Delta_{\mathrm{act}}$ becomes zero in Fig. 3. This indicates a close interrelation between δ_c and the magnitude of the Mott gap in the end compound. That is to say, δ_c increases in proportion with the transport gap in the end Mott insulator. On the basis of a simple three-dimensional Hubbard model that takes account of only the on-site Coulomb interaction, the system should become metallic with nonzero δ. The insulating phase with finite δ in $R_{1-x}\mathrm{Ca}_x\mathrm{TiO}_{3+y/2}$ is perhaps caused by some combined effect of the electron correlation and others (static disorder or electron-lattice interaction), which was discussed in Sec. III.

V. MAGNETIC PROPERTIES AND PHASE DIAGRAMS

The end compounds $R\mathrm{TiO}_3$ with relatively large ionic radius for R are known to show antiferromagnetism with slight

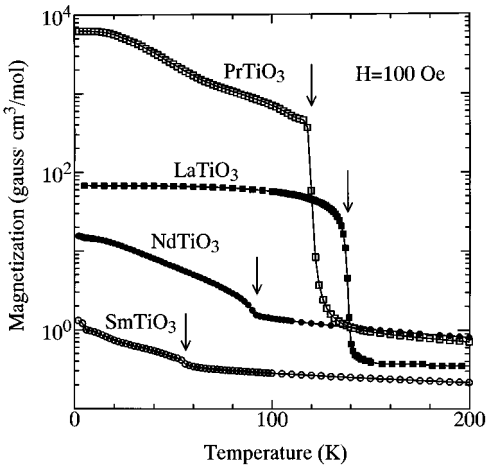

FIG. 5. Magnetization of $R\mathrm{TiO_3}$ at 100 Oe in a warming run, after the cooling the sample under 50 000 Oe. Arrows correspond to the antiferromagnetic ordering temperatures.

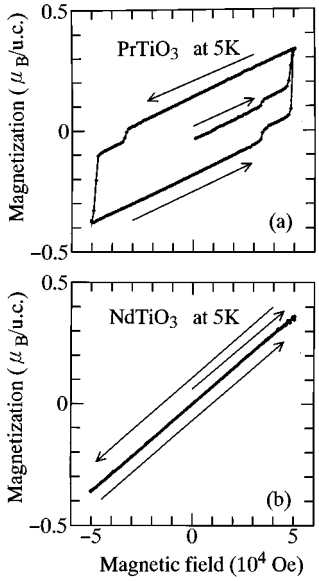

FIG. 7. Magnetization curves at 5 K measured at 100 Oe for (a) $\mathrm{PrTiO_3}$ and (b) $\mathrm{NdTiO_3}$.

spin-canting, giving rise to a small spontaneous magnetization.[14] To determine the antiferromagnetic (AF) ordering temperature T_N of each sample, magnetization measurements were carried out by the following procedure: The sample was first cooled down to 5 K with the application of a magnetic field of 50 000 Oe; then the magnetic field was decreased to 100 Oe, and the magnetization of the sample was measured in a warming run. The temperature dependence of the measured magnetization of $R\mathrm{TiO_3}$ is shown in Fig. 5, where T_N for each compound is indicated by an arrow. The results for $R=$La, Pr, and Nd are consistent with those previously reported.[8,15,12] As far as we know, the AF ordering of $\mathrm{SmTiO_3}$ is observed for the first time in the present study. On the other hand, $\mathrm{YTiO_3}$ shows a ferromagnetic ordering below $T_C \sim 30$ K.[10,14]

In Fig. 6 the magnetic-ordering temperatures of $R\mathrm{TiO_3}$ are plotted by closed circles together with the results reported by Greedan,[14] as a function of $\widetilde{W}^{-1}$. In the same figure results for $\mathrm{La_{1-x}Y_xTiO_3}$ from Refs. 25 and 7 are also plotted for comparison, where the Néel temperature (T_N) decreases with

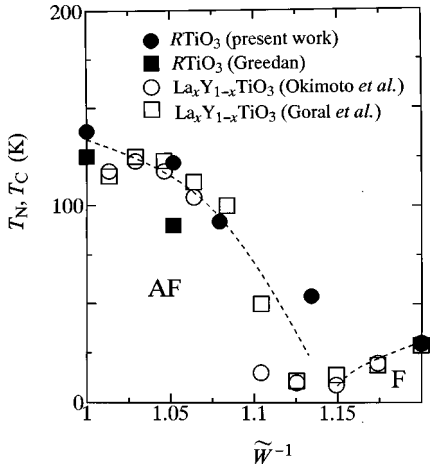

FIG. 6. Néel (T_N) and Curie (T_C) temperatures of $R\mathrm{TiO_3}$ (closed circles) and $\mathrm{La_xY_{1-x}TiO_3}$ (open circles) as a function of $\widetilde{W}^{-1}$. The data from literature (Refs. 7, 14, and 25) are also shown. The dashed lines are the guide to the eyes.

increase of Y concentration (increase of $\widetilde{W}^{-1}$) down to zero, and subsequently a ferromagnetic ordering appears and the Curie temperature (T_C) increases with a further increase of Y concentration. The result of $R\mathrm{TiO_3}$ in the present study also shows a similar behavior. However, it should be noted that a simple one-band Hubbard model hardly explains such a rapid decrease of T_N and the appearance of ferromagnetic ordering with an increase in $\widetilde{W}^{-1}$. In $R\mathrm{TiO_3}$, conduction electrons are accommodated in nearly triply degenerate Ti $3d$ t_{2g} orbitals, and the degenerate (multiband) Hubbard model seems appropriate to describe the experimental results. Recently, Mizokawa and Fujimori[26] investigated the spin structure of $R\mathrm{TiO_3}$ by a Hartree-Fock calculation, and found that ferromagnetic ordering is favored when the degeneracy of the $3d$ orbitals is taken into account. However, they claimed that the change of W alone does not explain the change of the spin structure from antiferromagnetic to ferromagnetic ordering, and that a Jahn-Teller distortion is important. In any case, the ferromagnetic ordering is accompanied by the ordering of the degenerate $3d$ orbitals. In fact, such an orbital ordering has recently been confirmed by polarized neutron-scattering experiments.[27] Moreover, a recent band calculation of $\mathrm{YTiO_3}$ (Ref. 28) by the generalized gradient approximation, taking account of its $\mathrm{GdFeO_3}$ distortion, succeeds in reproducing a ferromagnetic spin state with orbital ordering.

As shown in Fig. 5, the magnitude of the magnetization below T_N differs by several orders of magnitude depending on the species of R. We measured the magnetization curves at 5 K for $\mathrm{PrTiO_3}$ and $\mathrm{NdTiO_3}$ as shown in Fig. 7. For $\mathrm{PrTiO_3}$,[9] a large hysterisis was found with magnetic field, whereas almost no hysterisis was found for $\mathrm{NdTiO_3}$. Neutron-scattering measurements of these compounds indicate that $\mathrm{PrTiO_3}$ (Ref. 16) and $\mathrm{NdTiO_3}$ (Ref. 17) have qualitatively the same spin configuration both at the Ti site and the rare-earth site below T_N. At present it is not clear why the M-H curve below T_N behaves differently with different species of rare earth. We speculate, however, that such a

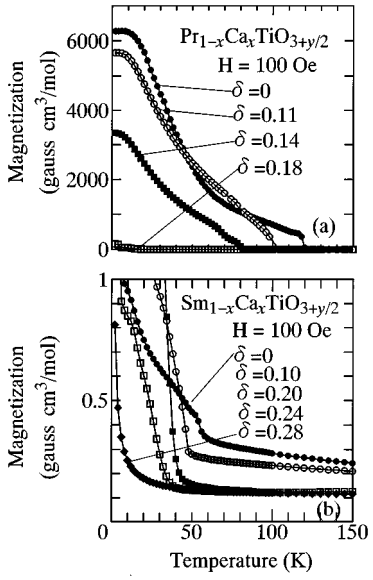

FIG. 8. Temperature dependence of magnetization for (a) $Pr_{1-x}Ca_xTiO_{3+y/2}$ and (b) $Sm_{1-x}Ca_xTiO_{3+y/2}$. The measurement condition is the same as in Fig. 5.

variety in the magnetism of $RTiO_3$ arises from the $3d$-$4f$ interaction between Ti and R.

We measured the magnetization of $R_{1-x}Ca_xTiO_{3+y/2}$ with finite $\delta(=x+y)$. The results for $Pr_{1-x}Ca_xTiO_{3+y/2}$ and $Sm_{1-x}Ca_xTiO_{3+y/2}$ are exemplified in Fig. 8. The magnetization of $Nd_{1-x}Ca_xTiO_3$ was also measured, and found to agree with that previously reported.[12] Irrespective of R, T_N decreases and finally disappears with an increase of δ for the respective compound. Figure 9 is a plot of T_N as a function of δ. Dashed lines correspond to the metal-insulator phase boundary determined by resistivity measurements, as described above. The AF phase extends to near the metal-insulator phase boundary for any R, which goes to a higher δ position in varying R from La to Sm. In other words, the AF phase survives as long as doped holes are localized. Such a correlation between the AF state and the carrier localization is also seen in cuprates such as $La_{2-x}Sr_xCuO_4$ (Ref. 3) and $R_{2-x}Ce_xCuO_4$,[29] and other transition-metal oxides such as $La_{1-x}Sr_xVO_3$.[30] This phenomenon is qualitatively understood as follows: If doped holes are localized, they will act as impurities with $S=0$, and such impurities do not effectively destroy the AF ordering as in a diluted spin system. But if a doped hole becomes movable, it will affect many sites with fairly short time scale, and will destroy the long-range AF ordering.

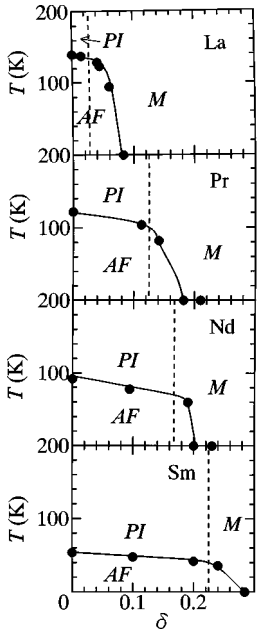

FIG. 9. Néel temperature for $R_{1-x}Ca_xTiO_{3+y/2}$ as a function of δ. The solid lines are the guide to the eyes. The dashed lines indicate the insulator-metal phase boundary determined from resistivity measurements.

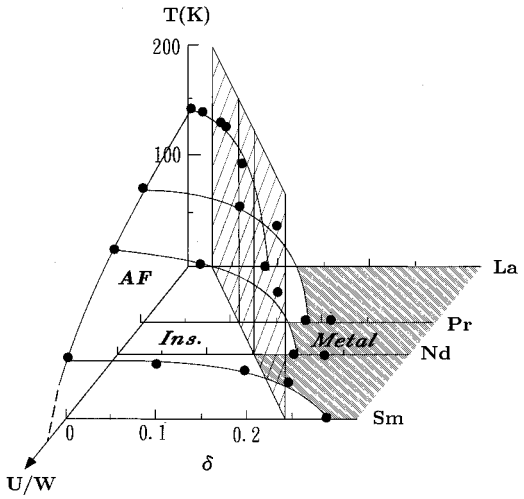

FIG. 10. The electronic phase diagram of $R_{1-x}Ca_xTiO_{3+y/2}$ in a space of the electron-correlation strength U/W, nominal hole concentration δ, and temperature T.

Figure 10 shows the electronic phase diagram of the present $R_{1-x}Ca_xTiO_{3+y/2}$ system as a function of U/W, $\delta=x+y$, and T. The T-U/W plane at $\delta=0$ indicates that T_N decreases with increase of correlation strength U/W for the end compound. The T-δ plane indicates that T_N decreases with an increase of hole concentration δ. The U/W-δ plane at $T=0$ indicates that both the insulating phase and the antiferromagnetic phase survive up to larger δ with larger U/W.

VI. BEHAVIOR NEAR PHASE BOUNDARIES

As seen in Fig. 9, there exits a metallic region where the AF state persists to at low temperature.[11] Figure 11 shows resistivity (ρ), the second T derivative of the resistivity ($d^2\rho/dT^2$), and magnetization (M) at 100 Oe (signaling the AF ordering with slight spin canting) for $Pr_{1-x}Ca_xTiO_{3+y/2}$ with $\delta=0.14$, as a typical example in such a region. T_N is $\sim$80 K for this sample, and the slope of $\rho(T)$ changes from positive to negative at this temperature. A sharp peak is observed for $d^2\rho/dT^2$ at the same temperature, indicating a steep change of the slope of $\rho(T)$ at T_N. In spite of such a critical change of resistivity with magnetic ordering, the resistivity does not diverge (i.e., the conductivity does not become zero) but remains finite at the lowest temperature (2 K) of the present measurement, as shown in the inset of Fig. 11

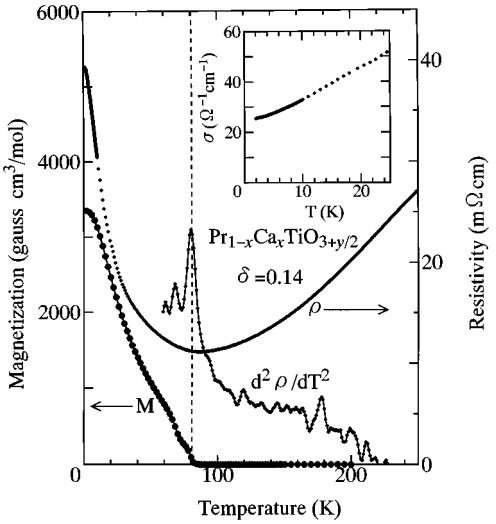

FIG. 11. Magnetization (M) at 100 Oe, resistivity (ρ), and second T derivative of ρ as a function of temperature (T) for $Pr_{1-x}Ca_xTiO_{3+y/2}$, with $\delta=0.14$.

where conductivity is plotted as a function of T. This indicates that the phase below 80 K is an AF *metallic* phase. Thus we may call this the transition from a high-temperature metal (HTM) to the low-temperature-antiferromagnetic metal (LTAFM). Such an AF metal has been observed for V_2O_3 with slight V vacancy,[31] where a spin-density wave with an incommensurate wave vector was observed by neutron diffraction.[32] It would be interesting to investigate whether such an incommensurate spin ordering also exists in these titanates.

The crystals near the border between the metallic phase and paramagnetic insulating (PI) phase also show a novel behavior. Figure 12 shows the temperature dependence of ρ for $Sm_{1-x}Ca_xTiO_{3+y/2}$ with $\delta=0.24$. The ρ value at room temperature is ~ 10 mΩ cm, and around 200 K it sharply decreases with decrease of temperature down to ~ 0.2 mΩ cm. Note that the temperature for the resistivity

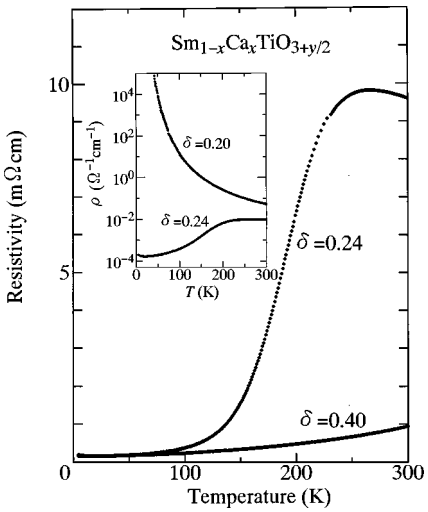

FIG. 12. Temperature (T) dependence of resistivity (ρ) for $Sm_{1-x}Ca_xTiO_{3+y/2}$ with $\delta=0.24$ and 0.40. The inset shows the T dependence of ρ for $Sm_{1-x}Ca_xTiO_{3+y/2}$ with $\delta=0.20$ and 0.24 on a logarithmic scale.

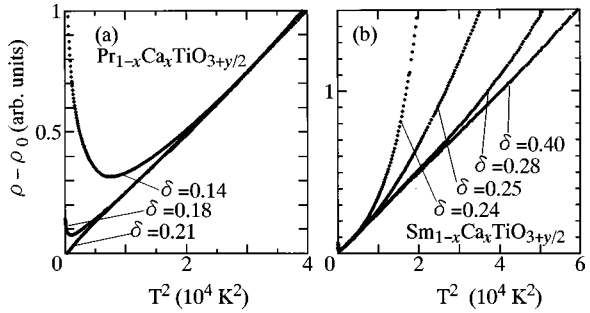

FIG. 13. $\rho-\rho_0$ vs T^2 for (a) $Pr_{1-x}Ca_xTiO_{3+y/2}$ and (b) $Sm_{1-x}Ca_xTiO_{3+y/2}$ with various δ. ρ_0 is the residual resistivity and the $\rho-\rho_0$ values are normalized, so that the slope becomes the same for all the data.

anomaly does not correspond to that of magnetic ordering, since T_N is much lower than this temperature. A similar resistivity change has also been observed for $Y_{1-x}Ca_xTiO_3$ with $x\sim 0.40$,[18] and these can be regarded as a transition from a high-temperature PI (HTPI) phase to low-temperature metallic (LTM) phase. Therefore, the phase boundary between the PI and metallic state shown by dashed lines in Figs. 9 and 10 is not completely parallel to the T axis, but is slightly inclined (going to larger δ with higher T). Such an electronic phase diagram is quite similar to those of V_2O_3 (Ref. 2) and $NiS_{2-x}Se_x$,[33] though the abscissa is different for these systems; namely, the band filling for $R_{1-x}Ca_xTiO_{3+y/2}$ and the bandwidth for V_2O_3 or $NiS_{2-x}Se_x$. Recent numerical calculations[19,34] based on the Hubbard model in infinite dimensions have reproduced the HTPI-LTM transition, which can be interpreted as the disappearance of the coherent peak in the density of states, which is responsible for the metallic conduction, with an increase in T.

In the metallic phase of $La_{1-x}Sr_xTiO_3$, the resistivity ρ follows T^2 relation from the lowest temperature to fairly high temperature (~ 300 K).[9] Such a T^2 dependence of the resistivity ρ is also observed for the metallic phases of other R systems. In the vicinity of the metal-insulator phase boundary; however, a deviation from this T^2 relation is observed. In Fig. 13 we plot ρ as a function of T^2. Here the residual resistivity (ρ_0) is subtracted, and the values of $\rho-\rho_0$ are normalized for the respective compounds, so that the slope appears the same. For $Pr_{1-x}Ca_xTiO_{3+y/2}$, the ρ value for $\delta=0.21$ shows a T^2 relation down to the lowest temperature, whereas, as δ decreases, ρ begins to deviate from the T^2 relation at low temperatures. This deviation is apparently related to the HTM-LTAFM transition described above. For $\delta=0.14$, T_N is 80 K (approximately corresponding to the temperature for the minimum resistivity) but the deviation from the T^2 relation is observable up to higher temperature ~ 140 K. This implies that strong antiferromagnetic fluctuations persist well above T_N in the doped system, which gives rise to an additional carrier-scattering process other than that contributing to the normal T^2 dependence. On the other hand, the deviation from the T^2 relation is observed for $Sm_{1-x}Ca_xTiO_{3+y/2}$ (and also $Y_{1-x}Ca_xTiO_{3+y/2}$) at higher temperatures, which would be related to the HTPI-LTM transition. For these smaller-W systems, the temperature range where ρ follows the T^2 relation is suppressed to

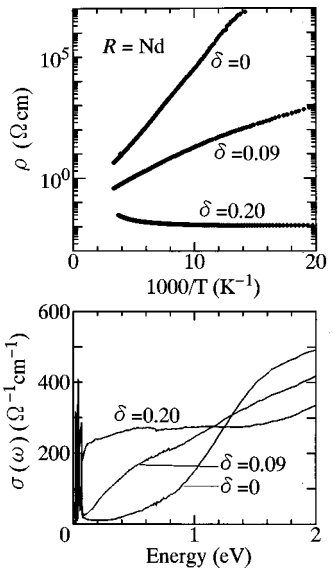

FIG. 14. (a) ρ vs T^{-1} for $Nd_{1-x}Ca_xTiO_{3+y/2}$ with $\delta=0$, 0.09, and 0.20, and (b) optical conductivity spectra $\sigma(\omega)$ for the corresponding crystals.

lower temperature as the system approaches the metal-insulator (MI) transition.

VII. INSULATING STATE WITH FINITE DOPING

As pointed out above, the insulating phase exists not only at half-filling but persists in the finite-doping region for the present Ti oxide. For example, in $Nd_{1-x}Ca_xTiO_{3+y/2}$, the $\delta=0$ sample shows thermal-activation-type carrier conduction, and a clear gaplike structure in the optical conductivity spectrum, as indicated in Fig. 14. Such an insulating state comes from the on-site Coulomb interaction (i.e., is a Mott insulator), as described above. When the 9% holes are doped to this Mott insulator, the resistivity keeps increasing with a decrease of temperature, but its temperature dependence deviates from the activation type.[35] In the optical conductivity spectrum,[5] the spectral weight increases inside the Mott-gap structure of the $\delta=0$ spectrum (forming the in-gap state), but the magnitude of the conductivity at zero energy remains almost zero. Such an insulating state, with a finite hole concentration, cannot be explained by a simple Hubbard model that takes account only of on-site Coulomb interaction. For the 18% doped sample, the resistivity decreases with a decrease of temperature, and the magnitude of conductivity at zero energy $[\sigma(\omega\sim0)]$ becomes finite, i.e., the sample is metallic, although the shape of $\sigma(\omega)$ is not a simple Drude-type. Such an insulating phase away from the integer filling is widely observed in other transition-metal oxides, such as perovskite-type vanadates[30] and manganites.[36]

Systematic optical studies of the present titanates[5] could clarify a characteristic feature of the insulating phase and the insulator-metal transition at fininte δ as follows. We define the spectral weight of the in-gap state,

$$N_{\mathrm{ingap}}=\frac{2m_0}{\pi e^2 N}\int_0^{\omega_c}\sigma(\omega)d\omega, \tag{1}$$

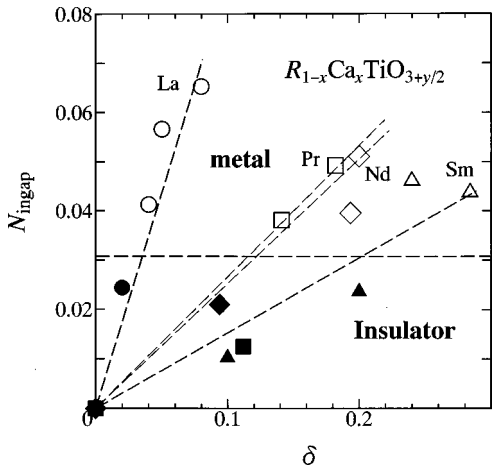

FIG. 15. Spectral weight of the in-gap state (N_{ingap}) as a function of δ for $R_{1-x}Ca_xTiO_{3+y/2}$. Closed symbols represent insulating crystals and open symbols the metallic ones. Circles, squares, rhombuses, and triangles represent $R=$La, Pr, Nd, and Sm, respectively. The dashed line indicates the critical value of N_{ingap} ($\sim$0.03) for the insulator-metal transition.

where m_0 is the free-electron mass, and N the number of Ti atoms per unit volume. The cut-off frequency ω_c is the isosbetic point of the spectra against the change of δ, which is 1.0–1.5 eV depending on the R species.[5] The N_{ingap} value proportionally increases with hole concentration,

$$N_{\mathrm{ingap}}=C\delta. \tag{2}$$

The coefficient C, i.e., the evolution rate of in-gap-spectral-weight, depends on the correlation strength of the system as

$$C\propto[(U/W)-(U/W)_c]^{-1}. \tag{3}$$

Such an in-gap state, however, does not contribute to the $\omega=0$ conduction, i.e., the system remains insulating, up to the critical hole concentration (δ_c) for the metal-insulator transition. The δ_c value depends on the strength of electron correlation (Fig. 4) approximately as

$$\delta_c\propto(U/W)-(U/W)_c. \tag{4}$$

In fact, the experimental value for $(U/W)_c$ in Eqs. (3) and (4) is nearly identical, as seen for the comparison between Figs. 3 and 4. Thus we can derive a simple law from these empirical relations,

$$N_c=C\delta_c=\mathrm{const.} \tag{5}$$

The value of N_c corresponds to the spectral weight of the in-gap state that is required for metallic conduction. In other words, the in-gap state caused by hole doping does not contribute to the metallic conduction if its spectral weight is less than a certain value. In Fig. 15, we plot N_{ingap} as a function of δ for several R. Here, we plot insulating samples (in which $d\rho/dT$ is negative at all temperatures) as closed symbols, and metallic ones as open symbols. This figure clearly shows the existence of the critical value N_c ($\sim$0.03) that separates the insulating and metallic regions, and does not depend on R, or the critical hole concentration δ_c.

Keeping such a feature in mind, let us consider the possible origin of the insulating state with finite doping. One

possibility is that the random potential might localize the conduction carriers, i.e., Anderson localization.[1] Such an effect is observed in doped semiconductors, where the dopant itself acts as a random potential and the sample remains insulating up to critical doping concentration. In the present $R_{1-x}Ca_xTiO_{3+y/2}$ system, the trivalent R and divalent Ca forms a solid solution, which could act as a random potential for the conduction carriers. Another possible origin for the insulating state is the electron-phonon interaction, by which conduction carriers could be localized as small polarons. In both cases, localization or delocalization of the conduction carriers depends on whether the transfer energy (bandwidth) for conduction carriers is smaller or larger than a critical value. In fact, Millis, Moeller, and Shraiman[37] recently investigated the effect of electron-phonon interaction on conduction carriers by a dynamical mean-field method, and found that the resistivity shows a semiconducting behavior when a dimensioless parameter $\lambda = g^2/kt$ (t is the transfer energy of electrons, g the coupling constant of electron-phonon interaction, and k the elastic force constant) is larger than a critical value. Such scenarios are consistent with the above-mentioned feature (existence of N_c), provided that the spectral weight of the in-gap state $N_{\rm ingap}$ represents the ''renormalized'' bandwidth for the carriers with strong electron correlation. In other words, doping controls such renormalized bandwidths, which increase proportionally with doping concentration, and the system becomes metallic when the hole concentration (the renormalized bandwidth) is larger than the critical value. Therefore, the in-gap spectral weight $N_{\rm ingap}$ measures the effective kinetic energy of the conduction carriers that governs their localization-delocalization transition.

Another possible candidate for the origin of the insulating state is the long-range Coulomb interaction, which would in cases induce the ordering of doped holes. This kind of hole ordering is in fact observed for the K_2NiF_4-type cuprate with $\frac{1}{8}$ hole concentration,[38] or for the K_2NiF_4-type nickelate with $\frac{1}{4}$,[39] $\frac{1}{3}$, and $\frac{1}{2}$ (Ref. 40) hole concentrations, but has not been observed for the present Ti oxides.

VIII. SUMMARY

We have investigated transport and magnetic properties of $R_{1-x}Ca_xTiO_{3+y/2}$ whose bandwidth (or strength of electron correlation) and band filling can both be controlled by the change of the (R, Ca) composition. The charge-gap magnitude (E_g) of the end compounds, $RTiO_3$, as well as the hole concentration required to make the sample metallic (δ_c), change with the correlation strength in a way that $\propto U/W-(U/W)_c$.

The Néel temperature (T_N) in $RTiO_3$ decreases from La to Sm (with decreasing bandwidth W), and $YTiO_3$ becomes a ferromagnet at low temperature. Such a decrease of T_N and the appearance of the ferromagnetism should be attributed to the degeneracy of the Ti $3d$ t_{2g} orbital as well as the orbital ordering. T_N also decreases with hole doping, but remains finite as long as the compound remains insulating.

The $R_{1-x}Ca_xTiO_{3+y/2}$ crystals near the MI phase boundary show characteristic behaviors. One is the transition from a high-temperature-metallic phase to a low-temperature-antiferromagnetic phase. The resistivity shows an upturn at the transition temperature but, its value remains finite at the lowest temperature (2 K in this experiment), indicating the existence of the antiferromagnetic metallic state. The other is the transition from a high-temperature-paramagnetic-insulating phase to a low-temperature-metallic phase. In both cases, a deviation from a T^2 dependence is observed for the resistivity in the metallic phases near the phase boundary. It was also found that the insulator-metal transition at a finite hole doping level in a series of $R_{1-x}Ca_xTiO_{3+y/2}$ takes place when the spectral weight of the in-gap state in the optical conductivity spectrum, which represents the effective kinetic energy of the mass-renormalized carriers, reaches the common critical value.

ACKNOWLEDGMENTS

We thank Y. Okimoto for his collaboration for the optical measurement and calculation of the bandwidth. We are also grateful to Y. Okada for his collaboration at the early stage of this study, and to M. Imada and N. Nagaosa for enlightening discussions. The present work was supported by a Grant-In-Aid for Scientific Research from Ministry of Education, Science, and Culture, Japan, and by NEDO.

[1] N. F. Mott, *The Metal-Insulator Transition* (Taylor and Francis, London, 1974).
[2] D. B. MacWhan, A. Menth, J. P. Remeika, W. F. Brinkman, and T. M. Rice, Phys. Rev. B **7**, 1920 (1973), and references therein.
[3] For example, H. Takagi, T. Ido, S. Ishibashi, M. Uota, S. Uchida, and Y. Tokura, Phys. Rev. B **40**, 2254 (1989).
[4] M. Imada, J. Phys. Soc. Jpn. **64**, 2954 (1995); M. A. Continentino, Phys. Rep. **239**, 178 (1994).
[5] T. Katsufuji, T. Okimoto, and Y. Tokura, Phys. Rev. Lett. **75**, 3497 (1995).
[6] D. A. Crandles, T. Timusk, J. D. Garett, and J. E. Greedan, Physica C **201**, 407 (1992).
[7] Y. Okimoto, T. Katsufuji, Y. Okada, T. Arima, and Y. Tokura, Phys. Rev. B **51**, 9581 (1995).
[8] F. Lichtenberg, D. Widmer, J. G. Bednorz, T. Williams, and A. Reller, Z. Phys. B **84**, 369 (1991).
[9] Y. Tokura, Y. Taguchi, Y. Okada, Y. Fujishima, T. Arima, K. Kumagai, and Y. Iye, Phys. Rev. Lett. **70**, 2126 (1993).
[10] Y. Taguchi, Y. Tokura, T. Arima, and F. Inaba, Phys. Rev. B **48**, 511 (1993).
[11] Y. Okada, T. Arima, Y. Tokura, C. Murayama, and N. Mori, Phys. Rev. B **48**, 9677 (1993).
[12] H. L. Ju, C. Eylem, J. L. Peng, B. W. Eichhorn, and R. L. Greene, Phys. Rev. B **49**, 13 335 (1994).
[13] D. A. MacLean, Hok-Nam Ng, and J. E. Greedan, J. Solid State Chem. **30**, 35 (1979).
[14] J. E. Greedan, J. Less-Common Met. **111**, 335 (1985).

[15] D. A. MacLean, K. Seto, and J. E. Greedan, J. Solid State Chem. **40**, 241 (1981).
[16] J. E. Greedan, J. Magn. Magn. Mater. **44**, 299 (1984).
[17] G. Amow and J. E. Greedan, J. Solid State Chem. **121**, 443 (1996).
[18] Y. Tokura, Y. Taguchi, Y. Moritomo, K. Kumagai, T. Suzuki, and Y. Iye, Phys. Rev. B **48**, 14 063 (1993).
[19] M. J. Rozenberg, G. Kotliar, and X. Y. Zhang, Phys. Rev. B **49**, 10 181 (1994).
[20] W. A. Harrison, *Electronic Structure and Properties of Solids* (Freeman, San Francisco, 1980).
[21] The tolerance factor of the perovskite structure is given by $t=(r_R+r_O)/[\sqrt{2}(r_{Ti}+r_O)]$, where r_R, r_{Ti}, and r_O are the ionic radii of the rare earth, titanium, and oxygen, respectively, which was tabulated by R. D. Shannon [Acta Crystallogr., Sect. A **32**, 751 (1976)]. Concerning the doped sample, we assume that r_R and r_{Ti} are the mean values of R and Ca, and Ti^{3+} and Ti^{4+}, respectively.
[22] A similar behavior has been reported for V_2O_3 with oxygen off-stoichiometry by G. A. Thomas *et al.* (Ref. 24). The authors claimed that the oxygen off-stoichiometry of V_2O_3 leads to the change of electron-correlation strength. It is apparent, however, that the oxygen off-stoichiometry also changes the valence of vanadium, i.e., the band filling of the crystal. The substitution of V by Ti or Cr (Ref. 2) should also have such a problem. In this sense, the doping in V_2O_3 would be more complicated than that of the present perovskite-type titanium oxides, where the change of the electron correlation and the band filling can be made independently.
[23] M. J. Rozenberg, X. Y. Zhang, and G. Kotliar, Phys. Rev. Lett. **69**, 1236 (1992); A. Georges and W. Krauth, *ibid.* **69**, 1240 (1992).
[24] G. A. Thomas *et al.*, Phys. Rev. Lett. **73**, 1529 (1994).
[25] J. P. Goral, J. E. Greedan, and D. A. MacLean, J. Solid State Chem. **43**, 244 (1982).
[26] T. Mizokawa and A. Fujimori, Phys. Rev. B **54**, 5368 (1996).
[27] J. Akimitsu *et al.* (unpublished).
[28] H. Sawada, N. Hamada, and K. Terakura, Physica B **237-238**, 46 (1997).
[29] G. M. Luke *et al.*, Nature (London) **338**, 49 (1989).
[30] F. Inaba, T. Arima, T. Ishikawa, T. Katsufuji, and Y. Tokura, Phys. Rev. B **52**, R2221 (1995).
[31] S. A. Carter, T. F. Rosenbaum, J. M. Honig, and J. Spalek, Phys. Rev. Lett. **67**, 3440 (1991).
[32] W. Bao, C. Broholm, S. A. Carter, T. F. Rosenbaum, G. Aeppli, S. F. Trevino, P. Metcalf, J. M. Honig, and J. Spalek, Phys. Rev. Lett. **71**, 766 (1993).
[33] J. A. Wilson, *The Metallic and Nonmetallic State of Matter*, edited by P. P. Edwards and C. N. R. Rao (Taylor and Francis, London, 1985), pp. 215–261; S. Miyasaka, H. Takagi, Y. Sekine, H. Takahashi, and N. Môri (unpublished).
[34] Th. Pruschke, D. L. Cox, and M. Jarrell, Phys. Rev. B **47**, 3553 (1993).
[35] The temperature dependence of the resistivity for the $\delta=0.09$ sample ($R=$Nd) can be fitted by the function $\rho(T)=\rho_0\exp(D/k_BT)^\alpha$ with $\alpha=0.6$ over six orders of a resistivity range. This function can also fit the data of $R=$Sm for $\delta=0.20$ with $\alpha=0.6-0.7$. Note that α should be $\frac{1}{4}$ according to a variable range hopping model in three-dimensional systems.
[36] A. Urushibara, Y. Moritomo, T. Arima, A. Asamitsu, G. Kido, and Y. Tokura, Phys. Rev. B **51**, 14 103 (1995).
[37] A. J. Millis, R. Mueller, and B. I. Shraiman, Phys. Rev. B **54**, 5389 (1996).
[38] J. M. Tranquada, B. J. Sternlieb, J. D. Axe, Y. Nakamura, and S. Uchida, Nature (London) **375**, 561 (1995).
[39] J. M. Tranquada, J. E. Lorenzo, D. J. Buttrey, and V. Sachan, Phys. Rev. B **52**, 3581 (1995).
[40] C. H. Chen, S-W. Cheong, and A. S. Cooper, Phys. Rev. Lett. **71**, 2461 (1993).